

Non-Stationary Vibratory Signatures Bearing Fault Detection Using Alternative Novel Kurtosis-based Statistical Analysis

Nur Adilla Kasim ^{a,*}, Mohd Ghafran Mohamed ^a and Mohd Zaki Nuawi ^b

^a Department of Mechanical Engineering, Politeknik Mukah, Mukah, Malaysia

^b Department of Mechanical and Material Engineering, Faculty of Engineering and Built Environment, Universiti Kebangsaan Malaysia, Bangi, Malaysia

Abstract

Vibration signature-based analysis to detect and diagnose is the commonly used technique in the monitoring of rotating machinery. Reliable features will determine the efficacy of diagnosis and prognosis results in the field of machine condition monitoring. This study intends to produce a reliable set of signal features through an alternative statistical characteristic before available relevant prediction methods. Given the above advantage of Kurtosis, a newly formed feature extraction analysis is adapted to extract a single coefficient out of EMD-based pre-processing vibration signal data for bearing fault detection monitoring. Each set of IMFs data is analyzed using the Z-rotation method to extract the data coefficient. Afterwards, the Z-rot coefficients, RZ are presented on the base of the specification of the defect vibratory signal to observe which IMF data set has the highest correlation over the specification given. Throughout the analysis studies, the RZ shows some significant non-linearity in the measured impact. For that reason, the Z-rotation method has effectively determined the strong correlation that existed in some of the IMFs components of the bearing fault. It corresponds to the first IMF for the inner race and the rolling ball specified a strong RZ coefficient with the highest correlation coefficient of $R^2 = 0.9653$ (1750 rpm) and $R^2 = 0.9518$ (1772 rpm), respectively. Whereas, the 4th IMF decomposition for the outer race bearing fault scored is $R^2 = 0.8865$ (1772 rpm). Meanwhile, the average R-squared score in the correlation between RZ coefficient and bearing fault throughout the study is $R^2 = 0.8915$. Thus, it can be utilized to be the alternative feature extraction findings for monitoring bearing conditions.

Keywords: Rotating machinery, Vibration signal, Bearing fault, statistical analysis, Z-rotation method

1. Introduction

Rolling element bearings are a crucial component in the rotating machinery assembly. The relative motion of the rolling elements becomes the primary sources for the elements to roll with sparse rolling friction. The dragging effect makes the rolling elements very fragile to develop fault and defects [1]. These defects create an undesirable vibration in the bearing, thus shortening the bearing life span and stabilizing equipment effectiveness. Therefore, it draws attention to researchers, engineers and manufacturers in machine condition monitoring. The rolling elements transmit forces for shaft revolution, it requires continuous monitoring, and any defect detection is compulsory to

* Corresponding author. Tel.: +60-192-613700; fax: +60-848-74005
E-mail address: ad11la@yahoo.com

Manuscript History:

Received 3 December, 2021, Revised 6 April, 2022, Accepted 21 April, 2022, Published 30 April, 2022

Copyright © 2021 UNIMAS Publisher. This is an open access article under the CC BY-NC-SA 4.0 license.

<https://doi.org/10.33736/jaspe.4594.2022>

avoid costly production downtime. Early fault diagnosis is necessary for safety and reliability improvement in the rotating machinery.

Bearing condition monitoring becomes an approach to studying the response of localized defects that may contain dents, pits, cracks, etc., through several deeds. Among the practice are monitoring the real-time changes until the running bearing becomes a failure, intentionally introducing defects in the bearing, shock wave examination, and applying statistical analysis to a time signal [2]. Vibration signature-based analysis for detection and diagnosis is the commonly used technique in the monitoring of rotating machinery. It offers an irregular revelation that formed on machinery components. A signal with crucial information can benefit a healthy or defective state for future planning action and preventive maintenance [3]. The signal acquisition from the rolling contact element generally examines the vibration level based (amplitude) on time and frequency domain transformation. While time-frequency domain analysis is preferably for a non-stationary vibration signal, outer race bearing fault is known to achieve a low correlation value. This is because the bearing elements vibrate more randomly as the defect becomes widespread and will develop higher clearance. Localized defects may yield the smoothness phenomena in the vibration kinematics, which reduces the signs of the periodic vibration [4]. The distinctive amplitude in bearing defect diminishes in exchange for the noise floor, or 'haystack' rises in the higher amplitude ranges.

Time-domain refers to a time function of the vibration data that often have comprehensive data regarding the inspection. The advantage of this domain is that it is never likely to result in erroneous analyses that include visual inspections, time wave formula, probability density function, and probability density moments. However, the downside is that there are sometimes excessive data for precise and straightforward faults diagnosis [2]. A time-domain form index is a solitary representative number calculated directly on the raw vibration signal, usually for trend lining and comparisons. The single-time formula comprises RMS, mean, peak value and peak to peak value has been applied with a low rate of defects detection rate [5]. A specific vibration signal amplitude range is possible to be presented using the probability density function. The function resembles a healthy bearing with a smooth bell shape curve of Gaussian (normal probability distribution). Some studies found it challenging to notice a fault in the displacement of time waveform. Therefore, they opted for other statistical analysis methods for failure analysis covering shape, impulse, a crest, and clearance factors.

In comparison, a probability density moment may bring the more informative index value such as mean, skewness and Kurtosis. Earlier, Kurtosis analysis is used to detect vibration magnitude impetuosity for defected bearing [6]. Other researchers have shown the usefulness of Kurtosis in bearing defect monitoring. Kurtosis is the most outstanding feature, which is sensitive to the impulsiveness in the vibration signal. Consequently, it is susceptible to distinguishing the vibration amplitude generated during bearing faults and recognition of defects. Since then, numerous studies have proven that Kurtosis is sensitive to signal shape, rotational speed, and signal frequency bandwidth [7]. However, those single time wave indices or statistical features may not ensure subsequent prediction accuracy [8] because of their miscellaneous pattern response from time to time due to the randomness of the vibration signal attribute.

The frequency domain is another analysis tool in signal processing by displaying the signal's energy distributed over the frequency range. While the time domain shows signal changes, the frequency domain presents a frequency spectrum as a signal representation. Fast Fourier Transform (FFT) is traditionally used as a transition medium to process the time domain into the frequency domain. The domain will display the natural frequency peaks of a spectrum of the repetitive vibration signal at the frequency where the repetition transpires. The elevation at the natural frequency will increase the vibration energy as the bearing produces a short duration pulse when encountering defects. Many researchers studied the rotational frequency and reported the success of bearing defect findings [2].

Further studies revealed prediction peaks in a discrete spectrum for inner race defects and the presence of the periodic and transmission path as a side-band around the defected-made peak under diverse loading for bearing defects [9]. Fourier-based analysis embodies some drawbacks, such as

signal decomposing being made into sinusoidal that may not be suitable for signal representation, linearity and stationary hypotheses. The spectral resolution is hardly local enough. For this reason, the time-frequency domain of short-time Fourier transform (STFT) is developed [10]. The STFT permits to harvest of meaningful time-frequency representations of non-stationary signals, and yet linear.

In contrast, the Wigner-Ville distribution (WVD) is concerned from time to time to lead the appearance of cross-terms. Alternatively, wavelet analysis (WA), discrete wavelet transform (DWT) and wavelet packet decomposition (WPA) allowed for expanding more accurate representation of the time-frequency in linear characteristics [11]. Rotating machinery monitoring principally deals with the non-linear and non-stationary signal where the time-frequency domain method is preferable. Empirical mode decomposition (EMD) and Hilbert-Huang transform (HHT) are popular tools for bearing fault detection and diagnosis [12]. Both time and frequency domains have been discovered for vibration signal presentation of bearing defects, and time-frequency analysis has been adopted to improve accuracy, enhance robustness, and reduce signal sensitivity to noise of the ratio [13].

Reliable features will determine the efficacy of diagnosis and prognosis results in the field of machine condition monitoring. Extracting features deceptively using the model is required rather than manually removing and selecting features. This study intends to produce a reliable set of signal features through an alternative statistical characteristic before available relevant prediction methods. Given the above advantage of Kurtosis, a newly formed feature extraction analysis was developed to extract a single coefficient out of EMD-based pre-processing vibration signal data for monitoring and detection of bearing faults.

2. Empirical Mode Decomposition (EMD)

Empirical mode decomposition decomposes a waveform into various components called intrinsic mode functions (IMF) [14]. Other analytic methods, like the Fourier transform and wavelet transform, can be compared to the motivation. It can be very local without assuming linearity, stationary, or any prior bases for decomposition. Because the decomposition is dependent on the data's local characteristic time scale, EMD is adaptable and efficient. It can be used to model non-stationary and non-linear processes. Using the EMD method, any complicated data collection can be broken down into a small number of discrete components. For the original signal, these components form a full and nearly orthogonal basis, which means that frequency energy is in the original signal.

The proposed signal will go through a sifting process called sifting, where the oscillation of riding waves can be abolished with no zero-crossing between extremes. The EMD algorithm will only consider very local signal oscillations. It divides the data into non-overlapping time scale components that obey two properties locally:

- a. Between two succeeding zero crossings, IMF has just one extreme, i.e. the differences between local minima and maxima are not more than one.
- b. The IMF's mean value is zero. It is worth noting that the second requirement implies that an IMF is stationary, making its study easier. An IMF, on the other hand, may contain amplitude modulation as well as altering frequency.

The following algorithm summarizes the sifting process. Decompose a data set $x(t)$ into IMFs $x_n(t)$ and a residuum $r(t)$ such that the signal can be represented as:

$$s(t) = \sum_n x_n(t) + r(t) \quad (21)$$

Shifting then means the following steps:

Step 0: Initialise: $n:=1, r_0(t)=x(t)$

Step 1: Extract the n -th IMF as follow:

- a. Affix $h_0(t) := r_{(n-1)}(t)$ and $k:=1$
 - b. Establish extreme of local maxima and minima of $h_{(k-1)}(t)$
 - c. Draw interpolation lines using splines, for $h_{(k-1)}(t)$, the upper (maxima) envelope $U_{(k-1)}(t)$ and lower (minims) envelope $L_{(k-1)}(t)$
 - d. Calculate the mean $m_{(k-1)}(t) = 1/2(U_{(k-1)}(t) + L_{(k-1)}(t))$ of both envelopes of $h_{(k-1)}(t)$. The low-frequency local trend is the name given to this running mean. A procedure is known as the ‘sifting’. It is used to determine the corresponding high-frequency local information.
 - e. Start, the k -th component $h_k(t) := h_{(k-1)}(t) - m_{(k-1)}(t)$.
 - If $h_k(t)$ has at least two extremes, increase $k \rightarrow k+1$ and repeat the sifting process from step (b),
 - If $h_k(t)$ satisfies the IMF criteria then set $x_n(t) := h_k(t)$ and $r_n(t) := r_{(n-1)}(t) - x_n(t)$
- Step 2: If $r_n(t)$ produces a residuum, stop the sifting process; if not, increase $n \rightarrow n+1$ and start at step 1 again.

3. Signal analysis using a novel statistical Z-rotation method

In the analysis of wear-signal amplitude correlation, reliable characteristics taken from raw signals are critical. [15]. The Z-rotation method was developed [16] based on the variance of a signal element dispersion around its mean centroid. The technique exhibits data patterns in defining the randomness of non-stationary time series data. It detects inferences and is expected to be more sensitive to variations in signal amplitude and anomalies. These interpretations are useful for forecasting and making decisions, such as in the machine learning adaption. The method initially begins with the gradual accumulation of signal components, but for this study, IMFs become the input data thus finding the mean value of each IMFs respectively. The following Eqn. 2 finds the variance between each element in the IMFs data by subtracting it from the earlier mean data [16].

$$r_i = |S_{n,i} - \bar{S}_y|_{i=1} \quad (2)$$

Statistical features of standard deviation, σ_r and Kurtosis, K_r become the key elements determining the RZ coefficient, as in Eqn. 2. Z-rot is a study of tracking To track the severity of a defect, utilize kurtosis. It is supposed to demonstrate a positive association over the defect progression.

$$RZ = \frac{1}{N} \sqrt{\sigma_r^4 K_r} \quad (3)$$

The duo reaction in the Z-rot method between standard deviation (sensitive to anomaly) and Kurtosis (sensitive to impulsiveness) is anticipated for the reliable coefficient of feature extraction to induce a high association between fault characteristics and signal features [16].

4. Methodology

After vibratory signals acquisition, the methodology approach consists of a complete empirical mode decomposition process directly on a signal without instantaneous frequency prior information. Figure 1 is the flow chart for this study to analyze and monitor Z-rot coefficient characteristics on the features of fault signals of rolling-element bearing monitoring. Residue from a sufficient number of repetitions allows the IMFs generations of the vibratory signal. Each set of IMFs data was analyzed using the Z-rot method to extract the data coefficient. Afterwards, the Z-rot coefficients were

presented on the base of the specification of the defect vibratory signal to observe which IMF data set had the highest correlation over the specification given.

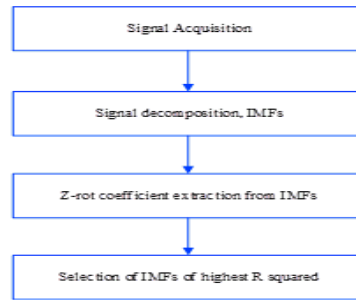


Figure 1. Research methodology

5. Vibration data

Vibratory signatures of rolling-element bearing vibration signals were downloaded from Case Western Reserve University Bearing Data Center. Some apparatus in the test stand, as in Figure 2, included an accelerometer, a 2 HP motor shaft supported by the test bearings and an electronics controller. Single point faults were intentionally introduced to test the Drive end SKF bearings with fault diameters of 0.175mm, 0.350mm, and 0.525mm. Magnetic based accelerometer was placed at the 12 o'clock position to the drive end housing and was collected at 48,000 samples per second. The transducer collected speed and horsepower data and was a handwritten record. The load directly affected the vibration response of the motor/bearing system. Therefore, static data for the outer raceway fault was placed at 6 o'clock for drive end bearing.

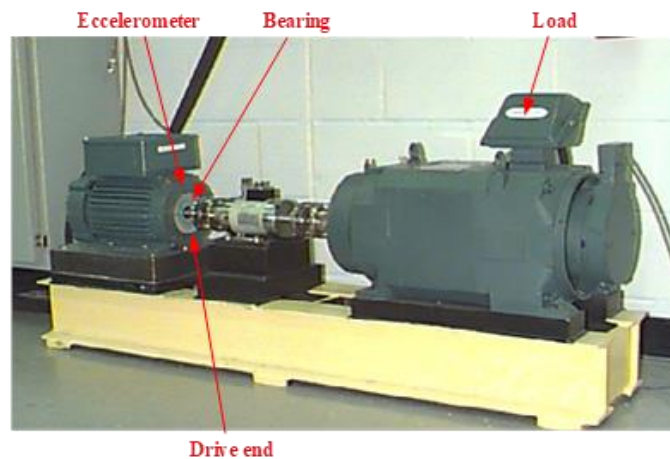


Figure 2. Schematic of bearing test apparatus

6. Results and discussion

The purpose of developing the Z-rotation method with a combination of different statistical moment levels was to have an alternative analytical method that could measure the actual risk in machining signals. As a result, there was a significant relationship with the development of bearing fault. This new method was expected to function stably under normal operation, especially after cutting passes the initial wear phase.

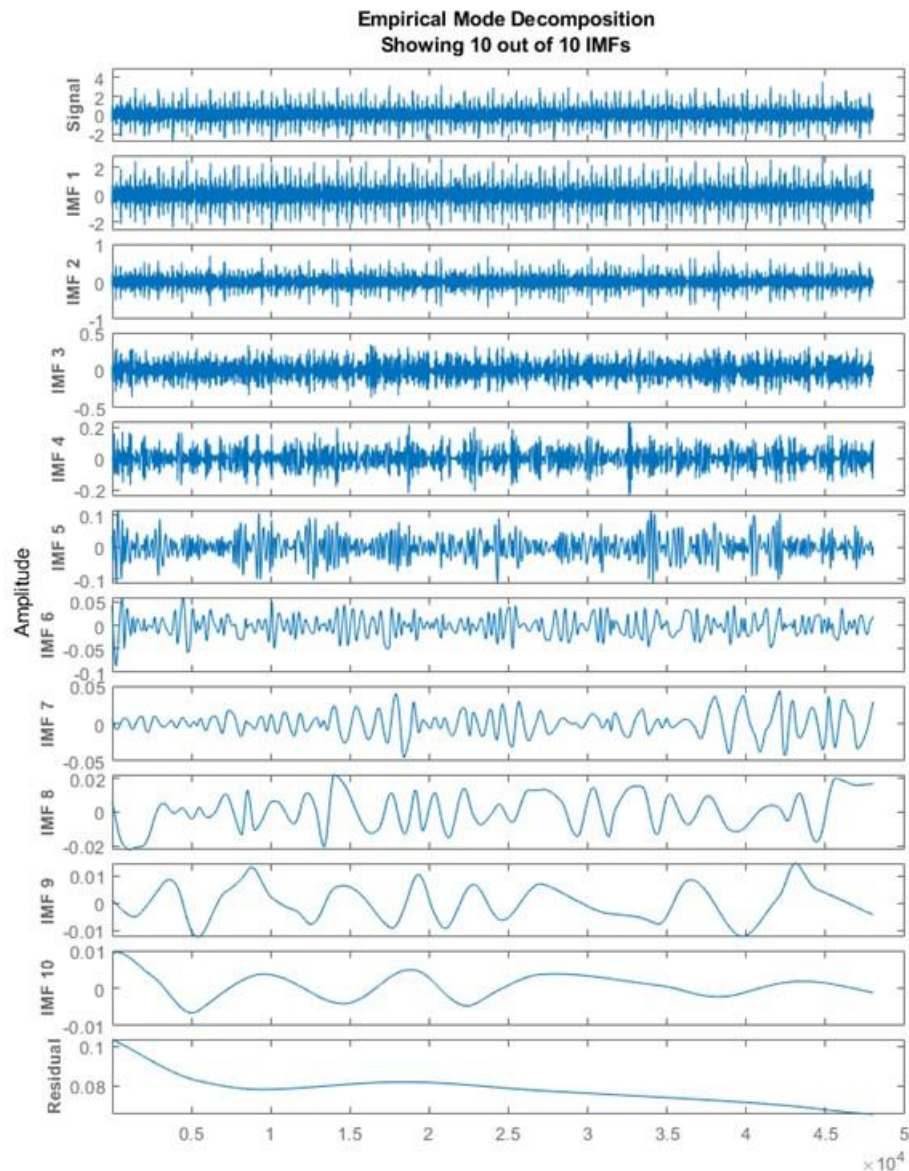


Figure 3. IMFs decomposition plot for sig_x109_DE_1797_0175_0_innerrace.

Under the previously described bearing fault condition, this study concentrated only on drive end accelerometer data with a sampling rate of 48000 Hz. They had a record total of 243938 data for 48K drive end bearing on the fault baseline without load, whereas data with the load was 486224 number. The data length was scaled down to smaller parts and had the equivalent statistical characterization with 132001:180000 and 240001:288000 segmented for no load and with load data, respectively. Subsequently, the interested number of data for each set was 48,000 and lengths to one second. The application of EDM took place on the segmented data and averagely generated 10 sets of IMF. MATLAB software was the platform to extract the IMFs data. Fig. 3 shows all IMFs compositions with the original vibratory signal and the residual. Overall, they were 397 observations to be analyzed using the Z-rot method. Table 1 shows the result of IMFs extracted from EMD for drive end accelerometer data.

Table 1. Number of decomposition

| Speed | | 1797 | 1772 | 1750 | 1730 |
|-------------------|--------------|-----------------------------|------|------|------|
| Load (hp) | | 0 | 1 | 2 | 3 |
| | Default (mm) | Number of IMF decomposition | | | |
| Baseline | | 10 | 10 | 10 | 10 |
| Inner race | 0.175 | 10 | 10 | 10 | 10 |
| | 0.350 | 10 | 10 | 10 | 10 |
| | 0.525 | 10 | 9 | 10 | 10 |
| Ball | 0.175 | 10 | 10 | 10 | 10 |
| | 0.350 | 10 | 10 | 10 | 10 |
| | 0.525 | 10 | 10 | 10 | 10 |

Statistical and spectral analysis are more presentable for successful diagnostic enhancement by reducing unwanted noise existing in the monitoring signal. Nevertheless, EMD is effectively a dyadic filter. Alternatively, it is possible to figure out which IMFs in a noisy collection carry information and which IMFs are pure noise. The first IMF usually carries the most oscillating high-frequency components. As for this study, consideration was made for all IMFs generated. Each IMF was analyzed using the Z-rot method. Table 2 shows the IMFs with the highest correlation according to fault progression, load and speed additions.

Table 2. Number of decomposition

| Speed | | 1797 | 1772 | 1750 | 1730 |
|-------------------|-------------------------|-------------------|---------------|---------------|---------------|
| Load (hp) | | 0 | 1 | 2 | 3 |
| | Default (mm) | R^Z coefficient | | | |
| Baseline | (1 st IMF) | 1.32E-07 | 1.32E-07 | 5.82E-07 | 5.82E-07 |
| Inner race | 0.175 | 1.40E-05 | 3.52E-06 | 3.51E-06 | 3.03E-06 |
| | 0.350 | 5.63E-05 | 5.84E-06 | 5.84E-06 | 5.26E-06 |
| | 0.525 | 1.45E-05 | 1.56E-05 | 2.33E-05 | 6.30E-06 |
| | R^2 | 0.7537 | 0.9539 | 0.9653 | 0.9551 |
| Baseline | (1 st IMF) | 1.32E-07 | 1.32E-07 | 5.82E-07 | 5.82E-07 |
| Ball | 0.175 | 7.08E-07 | 6.66E-07 | 6.85E-07 | 6.85E-07 |
| | 0.350 | 9.84E-07 | 2.52E-06 | 3.00E-06 | 3.18E-06 |
| | 0.525 | 4.07E-06 | 2.32E-06 | 9.82E-06 | 9.82E-06 |
| | R^2 | 0.9456 | 0.9518 | 0.8012 | 0.8055 |

Table 2 show R^Z coefficients for all relevant IMF suggest that the defect progression gave rise to the coefficient. As the fault became larger, an early bearing defect amplitude in time development was observed from the coefficient. Most of the coefficient and fault associations had a sturdy and robust correlation, with the average R squared scored 0.8915. For example, the inner race fault of the first IMF exhibited a strong correlation outcome of $R^2 = 0.9653$ (1750 rpm), where the higher the fault size, the R^Z values became progressive. The rolling ball in the bearing fault similarly corresponded to the first IMF, specifying a strong correlation between the RZ coefficient to score $R^2 = 0.9518$ (1772 rpm).

The newly developed Z-rot statistical signal feature in this experiment was analyzed alongside other global statistic features for efficiency verification and effectiveness. RMS, in general, has also been widely used in instrument condition monitoring because it can be an indication of the signal amplitude being in a constant or continuous state [17]. Researchers strongly favour Kurtosis analysis for monitoring and detecting failures on machine components [18]. As shown in Table 3, the Z-rot against RMS and Kurtosis achieved the highest correlation with an average R^2 of 0.8915 on three sets of experiments out of four sets of inner race fault. Meanwhile, RMS performed better results than Z-

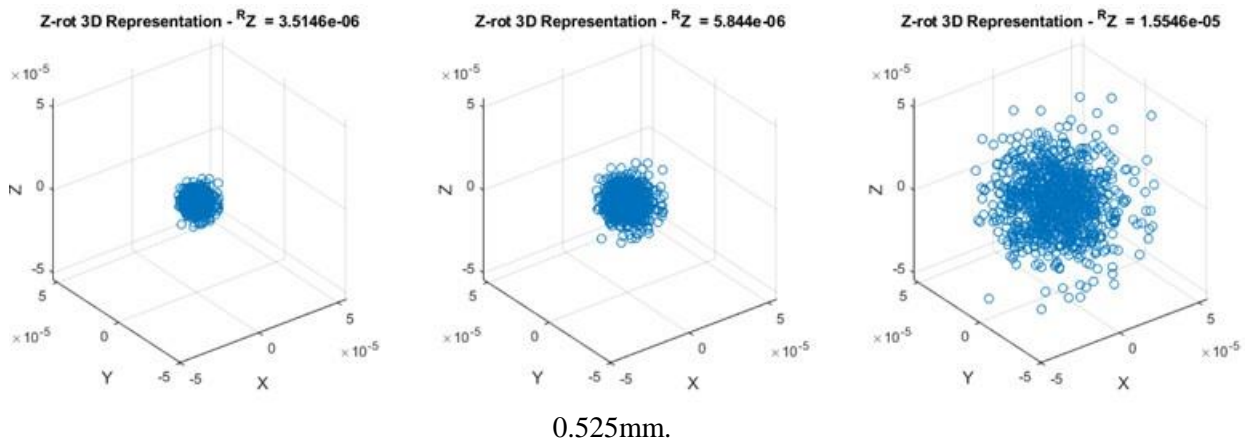
rot and Kurtosis with an average R^2 of 0.8938, especially for ball fault detection, where Z-rot still offered an excellent correlation. RMS got an additional score from all sets of experiments because the amplitude of the observed experimental test was changed more stably with the expansion of the fault [19].

Table 3. The comparison between Z-rot and other global statistics

| | Load, HP | Z-rot, R^2 | RMS, R^2 | Kurtosis, R^2 |
|----------------------------------|----------|---------------|---------------|-----------------|
| Inner race | 0 | 0.7537 | 0.7786 | 0.4343 |
| | 1 | 0.9539 | 0.9232 | 0.9671 |
| | 2 | 0.9653 | 0.8898 | 0.0584 |
| | 3 | 0.9551 | 0.9098 | 0.059 |
| Ball | 0 | 0.9456 | 0.7643 | 0.145 |
| | 1 | 0.9518 | 0.9713 | 0.4655 |
| | 2 | 0.8012 | 0.9483 | 0.5606 |
| | 3 | 0.8055 | 0.9654 | 0.5947 |
| Average, R^2 | | 0.8915 | 0.8938 | 0.4106 |

Meanwhile, the values of Kurtosis were not able to detect the amplitude of the increased vibration signal. This is because the amplitude increased at a uniform rate and had a comparative similarity to the average [20]. Therefore, the fourth-level statistical moment of individual kurtosis signal characteristics was less convenient because it was susceptible to impulsive signals. Nevertheless, the kurtosis feature in Z-rot allowed the coefficient to interact more effectively in signal amplitude changes that were unstable against the development of the bearing fault. Moreover, the standard deviation signal feature responded well to impulsive signals but not to RMS. Manipulating the best properties in standard deviation and kurtosis signal features helped the Z-rot extract signal features more effectively for gradual and unstable signals.

Figure 3. 3D graphic representation for the inner race fault spread from 0.175mm, 0.350mm and



The method provided a three-dimensional graphic representation and the Z-rot coefficient, RZ , which described the spread of data distribution. Figure 4 represents the scatter-degree of data distribution in the 3D dimension display. The 3D representation exhibited RZ for the bearing fault (0.175 mm) with a coefficient value of 3.5146e-06. The addition of sphere size as the coefficient value increased to 5.844e-06. As the fault size became more expansive, the analyzed coefficient value reached 1.5546e-05 for the inner race bearing fault.

3D graphics displayed a spread transformation from minor to more significant sphere

distribution. The spherical like distribution indicated the revolution of the R^Z coefficient regress with the more substantial bearing fault. All IMF sets demonstrated the same occurrence pattern distribution during research. Displays verified the helpfulness of the Z-rotation method as an alternative signal feature for the tracking procedure.

7. Conclusions

The goal of the Z-rotation method is to regress a relevant relationship between IMFs points with the element bearing fault. The technique through the coefficient has successfully detected the changes of bearing fault conditions over the increment of fault sizes. The analysis was done on the bearing fault vibration signal out of empirical mode decomposition. Throughout the analysis studies, the Z-rot coefficients showed some significant degree of non-linearity that appeared in the measured impact. For that reason, the Z-rotation method has effectively determined the strong correlation that existed in some of the IMFs components with the bearing fault. It corresponds to the first IMF for the inner race, and the rolling ball in the bearing fault specifies a strong R^Z coefficient with the highest correlation coefficient of $R^2 = 0.9653$ (1750 rpm) and $R^2 = 0.9518$ (1772 rpm), respectively. Meanwhile, the average R-squared in the correlation between R^Z coefficient and bearing fault throughout the study is $R^2 = 0.8915$. Thus, it can be utilized to be the alternative feature extraction findings for monitoring bearing conditions.

8. Research Highlights

- The bearing fault vibration signals are analyzed using an alternative statistical coefficient, R^Z .
- First IMF specifies a strong correlation between the R^Z coefficients.
- R^Z coefficient shows a strong correlation with the bearing fault progression.

Acknowledgements

The authors would like to thank Bearing Data Center, Case Western Reserve University, Cleveland, for providing us with the experimental data.

References

- [1] Fenineche, H., Felkaoui, A., & Rezig, A. (2019). Effect of input data on the neural networks performance applied in bearing fault diagnosis. *Rotating Machinery and Signal Processing* (pp. 34–43). Springer International Publishing. https://doi.org/10.1007/978-3-319-96181-1_3
- [2] Patil, M. S., Mathew, J., & RajendraKumar, P. K. (2007). Bearing signature analysis as a medium for fault detection: A review. *Journal of Tribology*, 130(1). <https://doi.org/10.1115/1.2805445>
- [3] Orhan, S., Aktürk, N., & Çelik, V. (2006). Vibration monitoring for defect diagnosis of rolling element bearings as a predictive maintenance tool: Comprehensive case studies. *NDT & E International*, 39(4), 293–298. <https://doi.org/https://doi.org/10.1016/j.ndteint.2005.08.008>
- [4] Williams, t., Ribadeneira, x., Billington, s., & Kurfess, t. (2001). Rolling element bearing diagnostics in run-to-failure lifetime testing. *Mechanical Systems and Signal Processing*, 15(5), 979–993. <https://doi.org/https://doi.org/10.1006/mssp.2001.1418>

- [5] Pham, D. T., & Oztemel, E. (1996). Condition monitoring and fault diagnosis. *Intelligent Quality Systems* (pp. 167–191). Springer London. https://doi.org/10.1007/978-1-4471-1498-7_8
- [6] Dyer, D., & Stewart, R. M. (1978). Detection of rolling element bearing damage by statistical vibration analysis. *Journal of Mechanical Design*, 100(2), 229–235. <https://doi.org/10.1115/1.3453905>
- [7] El-Thalji, I., & Jantunen, E. (2014). A descriptive model of wear evolution in rolling bearings. *Engineering Failure Analysis*, 45, 204–224. <https://doi.org/10.1016/j.engfailanal.2014.06.004>
- [8] Zhou, S., Xiao, M., Bartos, P., Filip, M., & Geng, G. (2020). Remaining useful life prediction and fault diagnosis of rolling bearings based on short-time fourier transform and convolutional neural network. *Shock and Vibration*, 2020, 8857307. <https://doi.org/10.1155/2020/8857307>
- [9] Su, Y.-T., & Lin, S.-J. (1992). On initial fault detection of a tapered roller bearing: Frequency domain analysis. *Journal of Sound and Vibration*, 155(1), 75–84. [https://doi.org/https://doi.org/10.1016/0022-460X\(92\)90646-F](https://doi.org/https://doi.org/10.1016/0022-460X(92)90646-F)
- [10] Kuo, R. ., & Cohen, P. . (1999). Multi-sensor integration for on-line tool wear estimation through radial basis function networks and fuzzy neural network. *Neural Networks*, 12(2), 355–370. [https://doi.org/10.1016/S0893-6080\(98\)00137-3](https://doi.org/10.1016/S0893-6080(98)00137-3)
- [11] Liu, J., Teng, G., & Hong, F. (2020). Human activity sensing with wireless signals: A survey. *Sensors*, 20(4). <https://doi.org/10.3390/s20041210>
- [12] Jia, F., Lei, Y., Lin, J., Zhou, X., & Lu, N. (2016). Deep neural networks: A promising tool for fault characteristic mining and intelligent diagnosis of rotating machinery with massive data. *Mechanical Systems and Signal Processing*, 72–73, 303–315. <https://doi.org/10.1016/j.ymsp.2015.10.025>
- [13] Zhang, X., Feng, N., Wang, Y., & Shen, Y. (2015). Acoustic emission detection of rail defect based on wavelet transform and Shannon entropy. *Journal of Sound and Vibration*, 339, 419–432. <https://doi.org/https://doi.org/10.1016/j.jsv.2014.11.021>
- [14] Huang, N. E., Shen, Z., Long, S. R., Wu, M. C., Shih, H. H., Zheng, Q., Yen, N.-C., Tung, C. C., & Liu, H. H. (1998). The empirical mode decomposition and the Hilbert Spectrum for nonlinear and non-stationary Time Series analysis. *Proceedings: Mathematical, Physical and Engineering Sciences*, 454(1971), 903–995. <http://www.jstor.org/stable/53161>
- [15] Krishnakumar, P., Rameshkumar, K., & Ramachandran, K. I. (2015). Tool Wear Condition prediction using vibration signals in high speed machining (HSM) of titanium (Ti-6Al-4V) alloy. *Procedia Computer Science*, 50, 270–275. <https://doi.org/10.1016/j.procs.2015.04.049>
- [16] Kasim, N. A., Nuawi, M., Ghani, J., Rizal, M., Ahmad, M. A. F., & Haron, C. (2019). Cutting tool wear progression index via signal element variance. *Journal of Mechanical Engineering and Sciences*, 13, 4596–4612. https://doi.org/10.15282/jmes.13.1.2019.17.0387_rfseq1
- [17] Abellan-Nebot, J. V., & Romero Subirón, F. (2010). A review of machining monitoring systems based on artificial intelligence process models. *The International Journal of Advanced Manufacturing Technology*, 47(1), 237–257. <https://doi.org/10.1007/s00170-009-2191-8>
- [18] Martin, H. R., & Honarvar, F. (1995). Application of statistical moments to bearing failure detection. *Applied Acoustics*, 44(1), 67–77. [https://doi.org/https://doi.org/10.1016/0003-682X\(94\)P4420-B](https://doi.org/https://doi.org/10.1016/0003-682X(94)P4420-B)
- [19] Ait-Amir, B., Pougnet, P., & El Hami, A. (2015). 6 - Meta-Model Development. In A. El Hami & P. Pougnet (Eds.), *Embedded Mechatronic Systems 2* (pp. 151–179). Elsevier. <https://doi.org/https://doi.org/10.1016/B978-1-78548-014-0.50006-2>
- [20] Nuawi, M. Z., Nor, M. J. M., Jamaludin, N., Abdullah, S., Lamin, F., & Nizwan, C. K. E. (2008). Development of integrated Kurtosis-based algorithm for Z-filter technique. *Journal of Applied Sciences*, 8(8), 1541–1547. <https://doi.org/10.3923/jas.2008.1541.1547>